City Research Online

City, University of London Institutional Repository

Original Investigation

Independent Modulation of Engagement and Connectivity of the Facial Network During Affect Processing by *CACNA1C* and *ANK3* Risk Genes for Bipolar Disorder

Danai Dima, PhD; Jigar Jogia, PhD; David Collier, PhD; Evangelos Vassos, MD, PhD; Katherine E. Burdick, PhD; Sophia Frangou, MD, PhD

IMPORTANCE Genome-wide association studies (GWASs) indicate that single-nucleotide polymorphisms in the *CACNA1C* and *ANK3* genes increase the risk for bipolar disorder (BD). The genes influence neuronal firing by modulating calcium and sodium channel functions, respectively. Both genes modulate γ-aminobutyric acid–transmitting interneuron function and can thus affect brain regional activation and interregional connectivity.

OBJECTIVE To determine whether the genetic risk for BD associated with 2 GWAS-supported risk single-nucleotide polymorphisms at *CACNA1C* rs1006737 and *ANK3* rs10994336 is mediated through changes in regional activation and interregional connectivity of the facial affect–processing network.

DESIGN, SETTING, AND PARTICIPANTS Cross-sectional functional magnetic resonance imaging study at a research institute of 41 euthymic patients with BD and 46 healthy participants, all of British white descent.

MAIN OUTCOMES AND MEASURES Blood oxygen level–dependent signal and effective connectivity measures during the facial affect–processing task.

RESULTS In healthy carriers, both genetic risk variants were independently associated with increased regional engagement throughout the facial affect–processing network and increased effective connectivity between the visual and ventral prefrontal cortical regions. In contrast, BD carriers of either genetic risk variant exhibited pronounced reduction in ventral prefrontal cortical activation and visual-prefrontal effective connectivity.

CONCLUSIONS AND RELEVANCE Our data demonstrate that the effect of *CACNA1C* rs1006737 and *ANK3* rs10994336 (or genetic variants in linkage disequilibrium) on the brain converges on the neural circuitry involved in affect processing and provides a mechanism linking BD to genome-wide genetic risk variants.

Author Affiliations: Section of Neurobiology of Psychosis, Department of Psychosis Studies, Institute of Psychiatry, King's College London, London, England (Dima, Jogia); Social Genetic and Developmental Psychiatry, Institute of Psychiatry, King's College London, London, England (Collier, Vassos); Department of Psychiatry, Icahn School of Medicine at Mt Sinai, New York, New York (Burdick, Frangou).

Corresponding Author: Sophia Frangou, MD, PhD, Department of Psychiatry, Icahn School of Medicine at Mount Sinai, 1425 Madison Ave, New York, NY 10029 (sophia.frangou @mssm.edu).

Bipolar disorder (BD) is characterized by mood dysregulation and a typically remitting-relapsing course.[1] Genome-wide association studies (GWASs) have successfully identified several common risk-conferring variants, including markers within the *CACNA1C* (HGNC 1390) and *ANK3* (HGNC 494) genes.[2,3]

The *CACNA1C* gene encodes the alpha subunit of the L-type voltage-dependent calcium (Ca^{+2}) channel Cav1.2. These channels mediate the influx of Ca^{+2} on membrane polarization, thus influencing neuronal ability to generate and transmit electrical signals.[4] In addition, the L-type Ca^{+2} channel subunit Cav1.2 contributes to the development and maturation of parvalbumin (PV) γ-aminobutyric acid–transmitting (GABAergic) interneurons.[5] The *ANK3* gene encodes ankyrin G, a cytoskeletal scaffolding protein located in the axon initial segment of neurons and in the nodes of Ranvier.[6] Ankyrin G determines action potential generation by the cooperative activation of sodium gated channels at the nodes of Ranvier[7] and promotes the formation of GABAergic synapses at the axon initial segment.[8] Of particular interest from the perspective of the neural systems is the link between *CACNA1C* and *ANK3* and the GABAergic interneurons. Brain oscillatory activity, considered a hallmark of neuronal network function,[9] crucially depends on GABAergic function.[10]

Thus, *CACNA1C* and *ANK3* may independently influence neuronal firing and coupling.

Functional magnetic resonance imaging (fMRI) studies have begun to uncover the effects of risk variants in *CACNA1C* and *ANK3* at the neural system level in healthy individuals. Research to date has focused on GWAS-supported single-nucleotide polymorphisms at *CACNA1C* rs1006737 (signal maximum at rs1006737; $P = 7.0 \times 10^{-8}$) and *ANK3* rs10994336 (signal maximum at rs10994336; $P = 9.1 \times 10^{-9}$).[2,3] Although intronic, these single-nucleotide polymorphisms are associated with altered gene expression in the brain.[11,12] The *CACNA1C* rs1006737 risk allele has been associated with overactivation of the amygdala (AMG)-hippocampal complex and the prefrontal cortex during cognitive and affect-processing tasks.[11,13-15] In addition, the *CACNA1C* rs1006737 risk allele influences connectivity between the right and left hippocampus[16] and between the prefrontal cortex and the AMG[17] and subcortical regions.[18] Genetic variation in *ANK3* may also influence prefrontal function[19] and occipital-prefrontal coupling.[20] These functional changes in the brain may underpin the association between either risk allele and increased behavioral reactivity to negative affective stimuli.[21] Therefore, *CACNA1C* and *ANK3* risk alleles may be relevant to reports of disease-associated dysfunction in engagement and connectivity between prefrontal regions with limbic[22-30] and occipital areas.[31]

In this study, we combined conventional Statistical Parametric Mapping (SPM) and dynamic causal modeling (DCM)[32] of fMRI data to define the functional consequences in the brain of *CACNA1C* rs1006737 and *ANK3* rs10994336 during affect processing in euthymic patients with BD compared with healthy individuals. Facial affect is processed mainly in a right-sided network that involves occipital and temporal regions of the ventral visual pathway within the inferior occipital gyrus (IOG), fusiform gyrus (FG), AMG, and ventral prefrontal cortex (VPFC).[33-35] We focused on this network primarily because it overlaps with regions implicated in BD.[36] Moreover, initial reports have confirmed that at least 1 of the risk alleles of interest, *CACNA1C* rs1006737, is functional within this network; in patients with BD, the presence of this risk allele amplifies frontolimbic abnormalities during facial affect processing.[15,18]

Based on this evidence, we tested the hypothesis that during facial affect processing, *CACNA1C* rs1006737 and *ANK3* rs10994336 risk variants will independently act to increase disease-related abnormalities in activation and effective connectivity within the facial affect-processing network. Specifically, we hypothesized that in patients with BD, the presence of either risk allele will increase neural responses in posterior facial affect-processing network regions while exacerbating abnormalities in activation and connectivity in ventral prefrontal regions.

Methods

Participants

Eighty-seven participants of self-reported white British ancestry were identified through departmental databases as part of ongoing studies on the pathophysiology of BD. Details of the

sample assessment are provided in the online material (Supplement [eMethods]). Forty-one euthymic patients with bipolar I disorder, diagnosed according to *DSM-IV* criteria,[1] were included in the study. Forty-six healthy individuals without a personal or a family history of Axis I *DSM-IV* disorders and matched to the patients on age, sex, and IQ (measured using the Wechsler Adult Intelligence Scale-Revised[37]) were selected as a control group. All participants underwent screening to exclude past, present, and hereditary medical disorders; *DSM-IV* lifetime alcohol or other drug dependence; alcohol or other drug abuse in the preceding 6 months; and contraindications to MRI. Psychopathology was assessed using the Hamilton Depression Rating Scale,[38] the Young Mania Rating Scale,[39] and the Brief Psychiatric Rating Scale (BPRS).[40]

The study was approved by the Joint South London and Maudsley and Institute of Psychiatry research ethics committee. All participants provided written informed consent before study participation.

DNA Extraction and Genotyping

We obtained DNA from the participants using buccal swabs and conventional procedures. The *CACNA1C* (rs1006737; risk allele A) and *ANK3* (rs10994336; risk allele T) genotypes were determined by an allelic discrimination assay (TaqMan Assay C_31344821_10; Applied Biosystems). End-point analysis was performed using fast real-time polymerase chain reaction analysis (7900HT; Applied Biosystems). Genotypes were called with the manufacturer's software (SDS, version 2.3; Applied Biosystems), and the output was checked visually to ensure genotypes fell into distinct clusters. The call rate was 100% because buccal swabs were repeated for 7 individuals for whom initial genotyping results were undetermined. Accuracy was assessed by duplicating 15% of the sample, and reproducibility was 100%.

Facial Affect Paradigm

The paradigm included 3 negative facial emotions (fear, anger, and sadness) in 3 separate experiments conducted in a single acquisition session in a randomized order. This paradigm consisted of 3 event-related tasks lasting 5 minutes each. In each task, 10 different facial identities (http://paulekman.com/) depicting 150% intensity of a negative (fear, anger, or sadness) or a neutral facial expression were presented in a pseudorandom order interspersed with a fixation cross. The 150% level of intensity was chosen to minimize ambiguity about the nature of the stimuli. The stimuli (affective and neutral faces and the fixation cross) were each displayed for 2 seconds and repeated 20 times. The interstimulus interval followed a Poisson distribution and varied between 3 and 9 (mean interval, 5) seconds. Participants were instructed to press the right or the left button with their dominant hand on an MRI-compatible response box to indicate whether the face had an emotional or a neutral expression. Response time and accuracy data were collected.

Image Acquisition

Anatomical and functional imaging data were acquired during the same session using a 1.5-T MRI system (GE Sigma; Gen-

eral Electric). Gradient-echo planar magnetic resonance (MR) images were acquired at each of the 16 noncontiguous planes parallel to the intercommissural (anterior commissure–posterior commissure) plane. We acquired T2*-weighted MR images reporting blood oxygenation level–dependent contrast (repetition time, 2000 milliseconds; echo time, 40 milliseconds; flip angle, 70°; section thickness, 7 mm; section skip, 0.7 mm; matrix size, 64 × 64; voxel dimensions, 3.75 × 3.75 × 7.7 mm). For each participant, 450 fMRIs were acquired. A high-resolution T1-weighted structural image was acquired in the axial plane for coregistration (inversion recovery-prepared, spoiled gradient-echo sequence; repetition time, 18 milliseconds; echo time, 5.1 milliseconds; inversion time, 450 milliseconds; flip angle, 20°; slice thickness, 1.5 mm; matrix size, 256 × 192; field of view, 240 × 180 mm; voxel dimensions, 0.9375 × 0.9375 × 1.5 mm; number of excitations, 1).

Statistical Parametric Mapping

Data analysis was implemented using SPM8 (www.fil.ion.ucl.ac.uk/spm/; Wellcome Trust Centre for Neuroimaging). Preprocessing involved spatial transformations (realignment and transformation into standard stereotactic Montreal Neurological Institute space using the participants' anatomical image) and smoothing with an isotropic gaussian kernel of 8 mm full-width half maximum. For each participant, the fMRI data from the 3 event-related tasks (fear, anger, or sadness vs neutral) were concatenated and modeled with a general linear (convolution) model. Vectors of onset representing correct responses were convolved with a canonical hemodynamic response function. Six movement parameters were also entered as nuisance covariates. The means of the 3 sessions were also modeled, as was the transition at the end of each session. For each participant, contrast images (affective > neutral facial expressions) were produced.

Group-level analyses were based on random-effects analyses of the single-subject contrast images using the summary statistic approach. Data were analyzed using 2 approaches. For each genetic variant, the primary hypothesis-testing analyses focused on the effect of the diagnosis, the genotype, and their interaction within volumes of interest (VOIs) defined within the facial affect–processing network, followed by whole-brain analyses to test for significant main effects or interactions outside the predefined areas.

Based on previous work from our laboratory,[35] we selected VOIs within the IOG, FG, AMG, and VPFC, which are the key brain regions engaged in facial processing. These VOIs were defined using a mask derived from the automated anatomical labeling atlas in Wake Forest University PickAtlas (version 3.0.3; www.fmri.wfubmc.edu/software/PickAtlas).

For the VOI and whole-brain analyses, statistical inference was based on a threshold of $P < .001$, uncorrected, with a voxelwise extent threshold of k = 20; in addition, for the VOI analysis, a small-volume correction was applied (VOI radius, 10 [measured as percentage of change in BOLD signal]; $P < .05$ at cluster level, familywise error).[41] We used response times and the BPRS total score as covariates in all analyses. The BPRS, Hamilton Depression Rating Scale, and Young Mania Rating Scale scores were highly correlated (for all, $R > 0.82$ [$P > .0001$]). To avoid collinearity, we used the total BPRS score as a covariate because, unlike the other scales, it is applicable to nonclinical populations. In the BPRS, symptoms are rated from 1 (absent) to 7 (extremely severe), with ratings below 4 corresponding to nonpathological experiences.

Measures of brain activation (weighted parameter estimates)[42] were extracted for each VOI from 1-sample t tests (contrast images affective > neutral facial expressions) for each diagnostic group using a region-of-interest toolbox for SPM (MarsBaR; http://marsbar.sourceforge.net). These measures were imported in commercially available software (SPSS, version 17; SPSS, Inc) to examine their association with task performance and with medication type and dose on the day of scanning.

Dynamic Causal Modeling

Dynamic causal modeling[32] is a Bayesian model comparison procedure that estimates directed interactions within neural systems. Crucially, DCM models these neural interactions and distinguishes between endogenous and context-specific coupling while accounting for the effects of experimentally controlled network perturbations (in contrast to stimulus-locked coupling).[32,43] In the previous study from our laboratory,[35] the strategy for determining the most parsimonious model for facial affect processing was detailed. In summary, a 4-area DCM was defined for all participants with endogenous connections between VOIs specified in the IOG, FG, AMG, and VPFC, with the main effect of all faces as the driving input to the IOG. We then produced and tested 7 models that included all possible permutations regarding how facial affect (fear, anger, or sadness) could modulate connections within the network (Supplement [eFigure]).

Model comparison was implemented using random-effects Bayesian model selection in DCM8 to compute exceedance and posterior probabilities at the group level[44] separately for controls and patients with BD. The exceedance probability of a given model denotes the probability that this model is more likely than any other model tested. To produce quantitative measures of the strength of effective connectivity and its modulation, we used random-effects Bayesian model averaging to obtain mean connectivity estimates (weighted by their posterior model probability) across all models and all subjects.[45] Once the optimal models for controls and patients were determined, we tested the modulation of the model connections by each of the risk variants separately in SPSS, version 17, using 2-sample t tests or nonparametric tests when data were not normally distributed based on the Kolmogorov-Smirnov criterion, with α = .05.

Results

Participants

Demographic and Clinical Data

Results for the *CACNA1C* rs1006737 (risk allele A) are shown in **Table 1**. Individuals with the *CACNA1C* AA allele (5 patients

Table 1. Demographic and Clinical Characteristics of the Study Participants by Diagnosis, *CACNA1C* Genotype (rs1006737; Risk Allele A), and Diagnosis×Genotype Interaction[a]

Characteristic	Effect of Diagnosis		Effect of *CACNA1C* Genotype		Diagnosis × Genotype Interaction			
	BD Patients (n = 41)	Controls (n = 46)	AA+AG (n = 42)	GG (n = 45)	BD Patients With AA+AG (n = 17)	Controls With AA+AG (n = 25)	BD Patients With GG (n = 24)	Controls With GG (n = 21)
Age, y	44.3 (11.9)	40.3 (13.2)	40.1 (11.1)	39.5 (12.4)	44.4 (12.3)	36.3 (10.4)	44.1 (11.6)	38.1 (13.4)
Sex, No. of participants								
Male	20	25	21	24	6	16	14	12
Female	21	21	21	21	11	9	10	9
Educational level	3.5 (1.0)	3.6 (1.0)	3.8 (0.9)	3.3 (1.0)	3.6 (0.9)	3.9 (0.9)	3.2 (1.0)	3.4 (1.0)
IQ	117.9 (17.9)	112.6 (14.5)	113.6 (18.4)	114.4 (13.0)	118.7 (20.2)	101.5 (12.5)	116.9 (14.5)	111.8 (17.2)
HDRS total score[b,c]	4.8 (5.3)	0.1 (0.5)	2.0 (3.5)	3.2 (5.5)	6.8 (6.5)	0.1 (0.5)	3.3 (3.8)	0.1 (0.5)
YMRS total score[b,c]	1.4 (3.0)	0.2 (0.6)	0.3 (0.7)	1.1 (2.7)	2.4 (3.5)	0.3 (0.6)	0.8 (2.3)	0.1 (0.7)
BPRS total score[b,c]	27.5 (4.0)	24.3 (0.7)	25.4 (2.1)	26.4 (4.2)	29.1 (5.0)	24.4 (0.7)	26.3 (2.6)	24.2 (0.6)
Age at onset, y	24.7 (8.0)	...	...	...	26.4 (9.3)	...	22.2 (4.7)	...
Duration of illness, y	20.2 (10.5)	...	...	...	19.0 (11.1)	...	21.9 (9.7)	...
No. of depressive episodes	5.7 (7.5)	...	...	...	4.7 (3.7)	...	7.9 (12.1)	...
No. of manic episodes	5.6 (7.7)	...	...	...	4.0 (3.5)	...	8.2 (11.5)	...
Correctly identified faces, %	90.3 (4.1)	93.1 (4.8)	91.7 (7.7)	91.7 (7.8)	90.9 (7.9)	92.9 (6.5)	89.4 (8.8)	93.3 (6.6)
Response time, ms[b]	1491 (209)	1109 (241)	1189 (267)	1171 (200)	1240 (249)	1125 (285)	1265 (236)	1097 (128)

Abbreviations: BD, bipolar disorder; BPRS, Brief Psychiatric Rating Scale; ellipses, not applicable; HDRS, Hamilton Depression Rating Scale; YMRS, Young Mania Rating Scale.

[a] Unless otherwise indicated, data are expressed as mean (SD).

[b] Scores for BD patients are significantly greater than those for controls ($P < .02$).

[c] Scores for BD patients in the AA+AG group are significantly greater than those for all other groups ($P < .03$).

Table 2. Demographic and Clinical Characteristics of the Study Participants by Diagnosis, *ANK3* Genotype (rs10994336; Risk Allele T), and Diagnosis×Genotype Interaction[a]

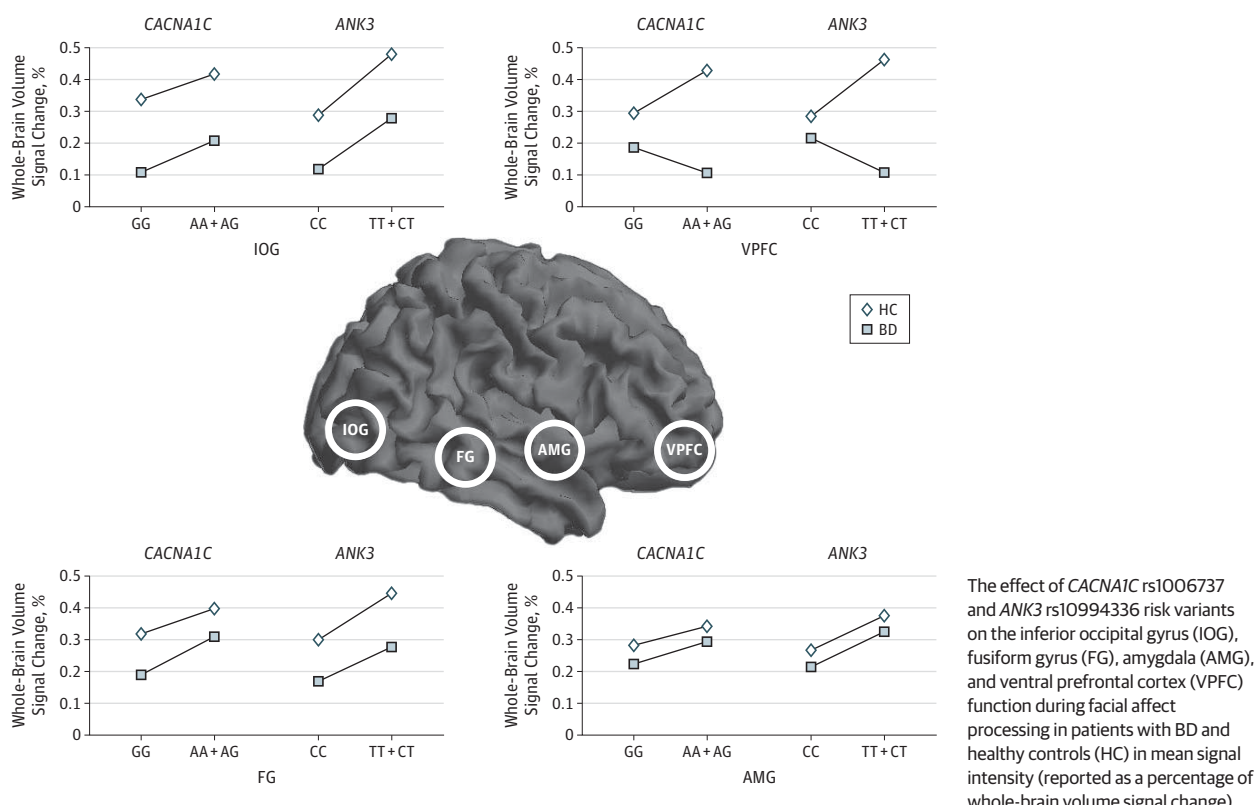| Characteristic	Effect of Diagnosis		Effect of *ANK3* Genotype		Diagnosis × Genotype Interaction			
	BD Patients (n = 41)	Controls (n = 46)	TT+CT (n = 30)	CC (n = 57)	BD Patients With TT+CT (n = 16)	Controls With TT+CT (n = 14)	BD Patients With CC (n = 25)	Controls With CC (n = 32)
Age, y	44.3 (11.9)	40.3 (13.2)	42.3 (13.0)	38.5 (13.4)	42.0 (10.7)	40.6 (12.2)	43.3 (12.3)	39.3 (12.3)
Sex, No. of Participants								
Male	20	25	17	27	9	7	11	18
Female	21	21	13	30	7	7	14	14
Educational level	3.5 (1.0)	3.6 (1.0)	3.5 (1.0)	3.5 (0.9)	3.5 (0.9)	4.2 (0.8)	3.1 (0.8)	3.6 (1.0)
IQ	117.9 (17.9)	112.6 (14.5)	121.7 (16.3)	111.8 (15.8)	112.3 (16.2)	110.7 (12.9)	121.7 (16.3)	116.7 (14.5)
HDRS total score[b,c]	4.8 (5.3)	0.1 (0.5)	2.9 (4.8)	0.5 (0.9)	5.3 (4.6)	0.4 (0.9)	1.5 (0.9)	0.1 (0.4)
YMRS total score[c,b]	1.4 (3.0)	0.2 (0.6)	0.8 (2.2)	0.1 (0.3)	1.6 (2.9)	0.2 (0.4)	0.7 (1.4)	0.2 (0.6)
BPRS total score[b,c]	27.5 (4.0)	24.3 (0.7)	26.2 (3.7)	24.6 (1.0)	27.3 (4.3)	24.8 (1.1)	25.9 (1.9)	24.2 (0.6)
Age at onset, y	24.7 (8.0)	...	...	...	23.3 (7.7)	...	21.5 (7.2)	...
Duration of illness, y	20.2 (10.5)	...	...	...	22.6 (9.0)	...	16.3 (10.7)	...
No. of depressive episodes	5.7 (7.5)	...	...	...	11.3 (14.0)	...	4.2 (3.8)	...
No. of manic episodes	5.6 (7.7)	...	...	...	12.2 (16.2)	...	3.7 (2.8)	...
Correctly identified faces, %	90.3 (4.1)	93.1 (4.8)	92.7 (5.9)	91.4 (8.3)	91.2 (6.2)	95.0 (4.1)	90.0 (9.4)	92.8 (7.0)
Response time, ms[b]	1491 (209)	1109 (241)	1223 (260)	1165 (231)	1244 (221)	1193 (328)	1252 (249)	1096 (185)

Abbreviations: BD, bipolar disorder; BPRS, Brief Psychiatric Rating Scale; ellipses, not applicable; HDRS, Hamilton Depression Rating Scale; YMRS, Young Mania Rating Scale.

[a] Unless otherwise indicated, data are expressed as mean (SD).

[b] Scores for BD patients are significantly greater than those for controls ($P < .02$).

[c] Scores for BD patients in the CT+TT group are significantly greater than those for all other groups ($P < .02$).

Figure 1. Effect of Bipolar Disorder (BD) Risk Genes on Facial Affect Processing

The effect of *CACNA1C* rs1006737 and *ANK3* rs10994336 risk variants on the inferior occipital gyrus (IOG), fusiform gyrus (FG), amygdala (AMG), and ventral prefrontal cortex (VPFC) function during facial affect processing in patients with BD and healthy controls (HC) in mean signal intensity (reported as a percentage of whole-brain volume signal change).

with BD and 4 controls) were considered together with AG heterozygotes (19 patients with BD and 17 controls) within each diagnostic group. Results for the *ANK3* rs10994336 (risk allele T) are presented in **Table 2**. Because of the rarity of the risk T allele (HapMap CEU minor allele frequency, 0.07; www.hapmap.org), individuals with TT (2 patients with BD and 1 control) and CT (14 patients with BD and 13 controls) alleles were considered together within each diagnostic group. We found no effect of either genotype or of the genotype × diagnosis interaction on demographic data (*P* > .11) or on clinical variables (*P* > .29) except for BD carriers of the *CACNA1C* or *ANK3* risk allele who had higher symptom scores compared with all other groups (*P* < .02). Similar behavioral changes have been observed in healthy carriers of either risk allele who report higher ratings of anxiety, anhedonia, and neuroticism.[16,21]

Task Performance
Details are shown in Tables 1 and 2. No significant effect of diagnosis, genotype, or their interaction was observed for accuracy (*P* > .63). Patients had longer mean response times compared with the controls, but no effect of genotype or of a genotype × diagnosis interaction was detected (*P* > .56).

Statistical Parametric Mapping
Processing of affective compared with neutral facial expressions was associated with enhanced activation throughout the relevant network in both diagnostic groups (Supplement [eTable]). However, compared with controls, patients with BD

(regardless of genotype) showed reduced activation in the visual cortex (IOG), temporal visual association cortex (FG), and the VPFC. The *CACNA1C* and *ANK3* risk alleles were independently associated with increased activation in the IOG, FG, and AMG in all participants regardless of diagnosis (**Figure 1**). A significant diagnosis × genotype interaction was noted in the VPFC. The presence of either risk allele was associated with increased VPFC activation in controls but reduced VPFC activation in patients with BD (Figure 1). The main effect of genotype and the genotype × diagnosis interaction observed in the VOI analyses remained significant in the whole-brain volume analyses. The latter analyses identified further regions with significant effect of genotype in the angular gyrus (x = −30, y = −54, z = 34 [*z* score, 3.34]) for carriers of the *CACNA1C* risk allele and the middle occipital gyrus (left: x = −26, y = −90, z = −4 [*z* score, 3.70]; right: x = 48, y = −66, z = −14 [*z* score, 3.68]) for carriers of the *ANK3* risk allele.

Dynamic Causal Modeling
Results are presented in **Figure 2**. For simplicity, we used a single modulatory term labeled *facial affect*. The models contain distinct modulatory inputs for fear, anger, and sadness, allowing us to test their individual influence on connectivity.

In the controls, we replicated the previous finding[35] that the optimal model for facial processing with an exceedance probability of 41% contains reciprocal connections among all 4 network areas (IOG, FG, AMG, and VPFC). Affect processing (regardless of valence or genotype) was associated with sig-
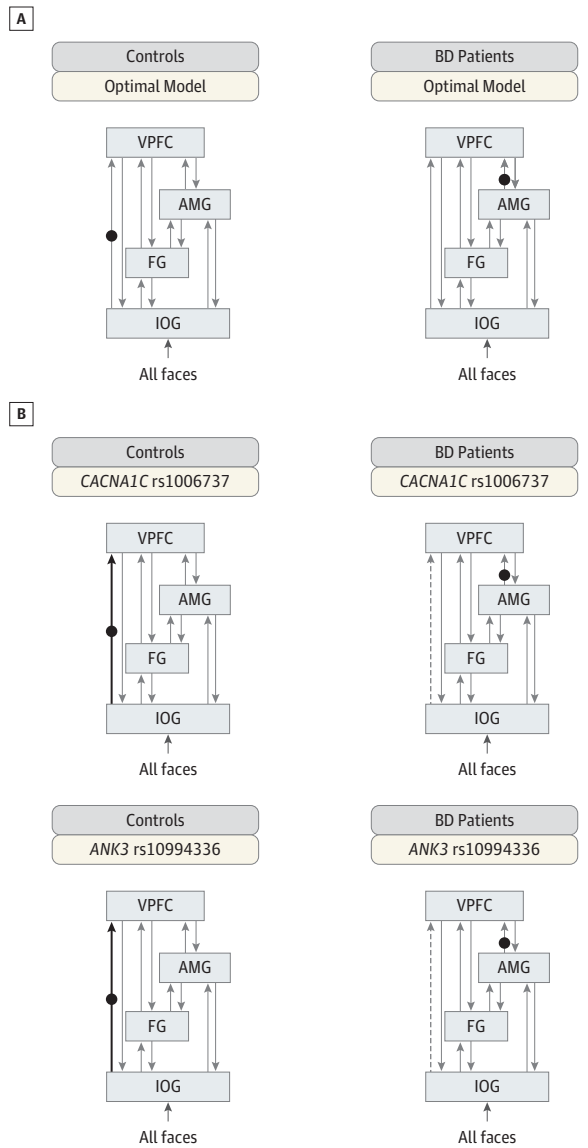
A, Optimal DCM selection. Models compromised by a 4-area DCM are specified
with bidirectional endogenous connections among all regions (inferior occipital
gyrus [IOG], fusiform gyrus [FG], amygdala [AMG], and ventral prefrontal cortex
[VPFC]) and a driving input of all faces into the IOG. For ease of display, affect
modulations are labeled as facial affect (**black dot**) but correspond to the
distinct modulations of fearful, angry, and sad faces. B, Alterations in effective
connectivity within the facial processing network established by Bayesian
model averaging across all models considered. For controls, the **bold black
arrows** indicate significantly increased connectivity from the IOG to the VPFC
modulated by the *CACNA1C* (rs1006737) and *ANK3* (rs10994336) risk variants.
For patients with BD, the **dashed arrows** indicate significantly decreased
connectivity from the IOG to the VPFC modulated by the *CACNA1C* (rs1006737)
and *ANK3* (rs10994336) risk variants. **Black solid arrows** indicate all other
network connections.

nificantly increased modulation of the forward connection
from the IOG to the VPFC (Figure 2A and Supplement [eFig-
ure, model 1]). In the controls, the presence of the *CACNA1C*

(P = .02) and ANK3 (P = .04) risk alleles further increased ef-
fective connectivity between these regions (Figure 2B).

In the patients with BD, as in the controls, the optimal
model with an exceedance probability of 32% also contained
reciprocal connections among all 4 network areas (IOG, FG,
AMG, and VPFC). Affect processing (regardless of valence or
genotype) was associated with reduced visual-prefrontal con-
nectivity coupled with increased modulation in the forward
connection from the AMG to the VPFC (Figure 2A and Supple-
ment [eFigure, model 3]). Moreover, BD carriers of the
CACNA1C (P = .02) or *ANK3* (P = .04) risk variant expressed fur-
ther reductions in connectivity from the IOG to the VPFC
(Figure 2B).

Differences between the 2 diagnostic groups were noted
in the modulation by facial affect of the IOG to VPFC (P = .02)
and AMG to VPFC (P = .03) connections. Furthermore, the
genotype × group interaction for the IOG to VPFC connection
was statistically significant for the *CACNA1C* (P = .003) and
ANK3 (P = .01) genotypes.

No significant effect of medication was found in any of the
analyses. In addition, no significant correlation between medi-
cation dose and any brain activation or connectivity param-
eters (P > .42) was found.

Discussion

We used SPM and DCM to investigate the effect of *CACNA1C*
and *ANK3* GWAS-supported risk variants on regional activa-
tion and interregional connectivity during facial affect pro-
cessing in healthy controls compared with euthymic patients
with BD. We found that both genetic risk variants were inde-
pendently associated with (1) increased engagement in the ven-
tral visual pathway and in the AMG irrespective of diagnosis,
(2) increased VPFC activation and visual-prefrontal effective
connectivity in controls, and (3) increased deviance in ven-
tral prefrontal activation and visual-prefrontal effective con-
nectivity in patients with BD.

The Effect of *CACNA1C* and *ANK3* Variation on the Facial
Affect–Processing Network in Controls
As expected,[35,46] facial affect processing enhanced regional ac-
tivation within the corresponding network regardless of geno-
type. The presence of either risk allele amplified these affect-
related neural responses. This genotype effect has been
reported previously in the AMG[14,15] and VPFC[15] for *CACNA1C*
rs1006737. Our study suggests that genetic modulation of re-
gional activation by *CACNA1C* rs1006737 within this network
is not limited to frontolimbic regions but extends to the ven-
tral visual pathway (IOG and FG). A similar pattern of affect-
related overactivation throughout the facial-processing net-
work was also present in *ANK3* rs10994336 risk allele carriers.

Regardless of genotype, optimal processing of visual
stimuli depends on visual-prefrontal cortical coupling. Spe-
cifically, visual cortical areas in the IOG rapidly project par-
tially analyzed information directly to the VPFC; this coarse
representation subsequently triggers predictions within
temporal regions (FG and AMG) about the most likely inter-

pretations of the stimulus.[47-49] When visual stimuli include affective information, this early visual-prefrontal coupling is further increased.[50] Accordingly, we found a robust modulation of effective connectivity between the IOG and VPFC by facial affect that was further enhanced in carriers of the *CACNA1C* rs1006737 or the *ANK3* rs10994336 risk allele. Therefore, one could argue that neural overresponsiveness to affective information could represent a common biological pathway shared by these 2 risk-conferring single-nucleotide polymorphisms for BD. This notion is further supported by neurophysiological evidence showing greater startle reactivity,[21] indicating increased neuronal excitability, in healthy carriers of either risk allele.

Although the underlying molecular mechanisms are beyond the resolution of neuroimaging, we hypothesize that the neurogenetic effects of either risk allele are mediated through changes in brain oscillatory activity. The functional coupling of visual and prefrontal cortices during visual processing relies on synchronized long-range oscillations within the gamma frequency band.[10,51] Recent optogenetic experiments have confirmed that gamma oscillations originate from PV-GABAergic interneurons following excitatory input from pyramidal cells.[10] The *CACNA1C* and *ANK3* genes are known to modulate neuronal firing, signaling, and PV-interneuron function, which are pertinent to the generation of gamma oscillations[4,5,7,8] and offer a plausible link between the molecular properties of the genes and their putative system-level effects observed here.

Effect of *CACNA1C* and *ANK3* Variation on the Facial Affect–Processing Network in BD

Regardless of genotype, patients with BD showed VPFC hypoactivation, consistent with previous reports.[26,27,52] This abnormality was exacerbated in BD carriers of either risk allele. In all other network regions, the presence of either risk allele amplified affect-related neural responses. This genotype-related imbalance in engagement between posterior facial network regions and the VPFC has been previously described for *CACNA1C* rs1006737.[15] Our findings suggest a similar effect for the *ANK3* rs10994336 risk allele.

Regardless of genotype, the patients with BD showed evidence of significant reduction in visual-prefrontal cortical effective connectivity but increased forward connectivity between the AMG and VPFC compared with the controls. These findings confirm previous reports of increased AMG-prefrontal coupling in BD[22-30] and provide new evidence of visual-prefrontal reduction in effective coupling. The latter was affected by *CACNA1C* and *ANK3* variation because BD carriers of either risk allele show greater dysfunction. Several reports have found abnormal neuronal synchronization in BD in the long-range gamma band during multiple tasks,[53-55] including facial affect processing,[56] that provides a plausible mecha-

nistic explanation for the observed reduction in visual-prefrontal cortical connectivity in BD.

Central Role of VPFC Dysfunction in the Pathophysiology of BD

Our results also strengthen the case for VPFC pathology in the pathogenesis of BD.[57] Postmortem studies in BD report neuropathological abnormalities in the VPFC, leading to regional reductions in the number and density of pyramidal cells and PV interneurons.[58,59] The mechanisms involved are not established, but multiple lines of evidence implicate reduced expression of neurotrophins,[60] abnormalities in oxidative energy generation,[60,61] and mitochondrial dysfunction resulting in altered Ca^{+2} regulation[60] and PV-interneuron reduction.[62] Given the known properties of the *CACNA1C* and *ANK3* risk alleles discussed here, we postulate that the risk alleles may further reduce the integrity of the interactions between excitatory signals from pyramidal neurons and inhibition by GABAergic interneurons.[10,63] A more precise formulation of a pathophysiological model for BD crucially depends on the future availability of data directly testing these predictions.

Methodological Considerations

Several methodological issues require further consideration. First, possible medication effects on the study results cannot be conclusively refuted. However, we found no significant relationship between medication and measures of regional activation or effective connectivity. Second, we did not test for epistatic effects because the number of individuals carrying both risk variants was small (3 patients and 3 controls). This finding is expected, given the rarity of the *ANK3* risk allele. However, Moskvina and colleagues[64] found no convincing evidence of epistasis between the GWAS-supported single-nucleotide polymorphisms in *ANK3* and *CACNA1C* in the Wellcome Trust Case Control Consortium data (1868 cases with BD and 2938 controls). They suggested that GWAS-supported loci may be detectable because they do not require interactions to exert an effect. Finally, the absence of a diagnosis or a genotype effect on task performance is a particular strength of the study and confirms the increased assay sensitivity of neuroimaging in uncovering the neural correlates of diagnostic and genetic variability. The genetic risk factors examined here and the results obtained show at least partial overlap with findings in other disorders, primarily schizophrenia.[59,65] This observation adds to accumulating evidence that the diagnostic categories used in clinical practice are unlikely to represent underlying genetic and pathophysiological risk accurately.

In summary, we demonstrated that the effect of *CACNA1C* rs1006737 and *ANK3* rs10994336 (or genetic variants in linkage disequilibrium) on the brain converges on neural circuitry involved in facial affect processing. Thus, we provide a mechanism linking BD with genome-wide genetic risk variants.

REFERENCES

1. American Psychiatric Association. *Diagnostic and Statistical Manual of Mental Disorders.* ed 4. Washington, DC: American Psychiatric Association; 1994.

2. Ferreira MA, O'Donovan MC, Meng YA, et al; Wellcome Trust Case Control Consortium. Collaborative genome-wide association analysis supports a role for *ANK3* and *CACNA1C* in bipolar disorder. *Nat Genet*. 2008;40(9):1056-1058.

3. Sklar P, Ripke S, Scott LJ, et al; Psychiatric GWAS Consortium Bipolar Disorder Working Group. Large-scale genome-wide association analysis of bipolar disorder identifies a new susceptibility locus near *ODZ4* [published correction appears in *Nat Genet*. 2012;44(9):1072]. *Nat Genet*. 2011;43(10):977-983.

4. Moosmang S, Lenhardt P, Haider N, Hofmann F, Wegener JW. Mouse models to study L-type calcium channel function. *Pharmacol Ther*. 2005;106(3):347-355.

5. Jiang M, Swann JW. A role for L-type calcium channels in the maturation of parvalbumin-containing hippocampal interneurons. *Neuroscience*. 2005;135(3):839-850.

6. Lambert S, Davis JQ, Bennett V. Morphogenesis of the node of Ranvier: co-clusters of ankyrin and ankyrin-binding integral proteins define early developmental intermediates. *J Neurosci*. 1997;17(18):7025-7036.

7. Zhou D, Lambert S, Malen PL, Carpenter S, Boland LM, Bennett V. AnkyrinG is required for clustering of voltage-gated Na channels at axon initial segments and for normal action potential firing. *J Cell Biol*. 1998;143(5):1295-1304.

8. Ango F, di Cristo G, Higashiyama H, Bennett V, Wu P, Huang ZJ. Ankyrin-based subcellular gradient of neurofascin, an immunoglobulin family protein, directs GABAergic innervation at Purkinje axon initial segment. *Cell*. 2004;119(2):257-272.

9. Buzsáki G, Draguhn A. Neuronal oscillations in cortical networks. *Science*. 2004;304(5679):1926-1929.

10. Sohal VS. Insights into cortical oscillations arising from optogenetic studies. *Biol Psychiatry*. 2012;71(12):1039-1045.

11. Bigos KL, Mattay VS, Callicott JH, et al. Genetic variation in *CACNA1C* affects brain circuitries related to mental illness. *Arch Gen Psychiatry*. 2010;67(9):939-945.

12. Rueckert EH, Barker D, Ruderfer D, et al. *Cis*-acting regulation of brain-specific *ANK3* gene expression by a genetic variant associated with bipolar disorder. *Mol Psychiatry*. 2013;18(8):922-929.

13. Krug A, Nieratschker V, Markov V, et al. Effect of *CACNA1C* rs1006737 on neural correlates of verbal fluency in healthy individuals. *Neuroimage*. 2010;49(2):1831-1836.

14. Wessa M, Linke J, Witt SH, et al. The *CACNA1C* risk variant for bipolar disorder influences limbic activity. *Mol Psychiatry*. 2010;15(12):1126-1127.

15. Jogia J, Ruberto G, Lelli-Chiesa G, et al. The impact of the *CACNA1C* gene polymorphism on frontolimbic function in bipolar disorder. *Mol Psychiatry*. 2011;16(11):1070-1071.

16. Erk S, Meyer-Lindenberg A, Schnell K, et al. Brain function in carriers of a genome-wide supported bipolar disorder variant. *Arch Gen Psychiatry*. 2010;67(8):803-811.

17. Wang F, McIntosh AM, He Y, Gelernter J, Blumberg HP. The association of genetic variation in *CACNA1C* with structure and function of a frontotemporal system. *Bipolar Disord*. 2011;13(7-8):696-700.

18. Radua J, Surguladze SA, Marshall N, et al. The impact of *CACNA1C* allelic variation on effective connectivity during emotional processing in bipolar disorder. *Mol Psychiatry*. 2013;18(5):526-527.

19. Roussos P, Katsel P, Davis KL, et al. Molecular and genetic evidence for abnormalities in the nodes of Ranvier in schizophrenia. *Arch Gen Psychiatry*. 2012;69(1):7-15.

20. Ruberto G, Vassos E, Lewis CM, et al. The cognitive impact of the *ANK3* risk variant for bipolar disorder: initial evidence of selectivity to signal detection during sustained attention. *PLoS One*. 2011;6(1):e16671. doi:10.1371/journal.pone.0016671.

21. Roussos P, Giakoumaki SG, Georgakopoulos A, Robakis NK, Bitsios P. The *CACNA1C* and *ANK3* risk alleles impact on affective personality traits and startle reactivity but not on cognition or gating in healthy males. *Bipolar Disord*. 2011;13(3):250-259.

22. Foland LC, Altshuler LL, Bookheimer SY, Eisenberger N, Townsend J, Thompson PM. Evidence for deficient modulation of amygdala response by prefrontal cortex in bipolar mania. *Psychiatry Res*. 2008;162(1):27-37.

23. Almeida JR, Versace A, Mechelli A, et al. Abnormal amygdala-prefrontal effective connectivity to happy faces differentiates bipolar from major depression. *Biol Psychiatry*. 2009;66(5):451-459.

24. Versace A, Thompson WK, Zhou D, et al. Abnormal left and right amygdala-orbitofrontal cortical functional connectivity to emotional faces: state versus trait vulnerability markers of depression in bipolar disorder. *Biol Psychiatry*. 2010;67(5):422-431.

25. Chepenik LG, Raffo M, Hampson M, et al. Functional connectivity between ventral prefrontal cortex and amygdala at low frequency in the resting state in bipolar disorder. *Psychiatry Res*. 2010;182(3):207-210.

26. Chen CH, Suckling J, Lennox BR, Ooi C, Bullmore ET. A quantitative meta-analysis of fMRI studies in bipolar disorder. *Bipolar Disord*. 2011;13(1):1-15.

27. Houenou J, Frommberger J, Carde S, et al. Neuroimaging-based markers of bipolar disorder: evidence from two meta-analyses. *J Affect Disord*. 2011;132(3):344-355.

28. Cerullo MA, Fleck DE, Eliassen JC, et al. A longitudinal functional connectivity analysis of the amygdala in bipolar I disorder across mood states. *Bipolar Disord*. 2012;14(2):175-184.

29. Delvecchio G, Fossati P, Boyer P, et al. Common and distinct neural correlates of emotional processing in bipolar disorder and major depressive disorder: a voxel-based meta-analysis of functional magnetic resonance imaging studies. *Eur Neuropsychopharmacol*. 2012;22(2):100-113.

30. Perlman SB, Almeida JR, Kronhaus DM, et al. Amygdala activity and prefrontal cortex–amygdala effective connectivity to emerging emotional faces distinguish remitted and depressed mood states in bipolar disorder. *Bipolar Disord*. 2012;14(2):162-174.

31. Pavuluri MN, O'Connor MM, Harral E, Sweeney JA. Affective neural circuitry during facial emotion processing in pediatric bipolar disorder. *Biol Psychiatry*. 2007;62(2):158-167.

32. Friston KJ, Harrison L, Penny W. Dynamic causal modelling. *Neuroimage*. 2003;19(4):1273-1302.

33. Fairhall SL, Ishai A. Effective connectivity within the distributed cortical network for face perception. *Cereb Cortex*. 2007;17(10):2400-2406.

34. Vuilleumier P, Driver J. Modulation of visual processing by attention and emotion: windows on causal interactions between human brain regions. *Philos Trans R Soc Lond B Biol Sci*. 2007;362(1481):837-855.

35. Dima D, Stephan KE, Roiser JP, Friston KJ, Frangou S. Effective connectivity during processing of facial affect: evidence for multiple parallel pathways. *J Neurosci*. 2011;31(40):14378-14385.

36. Strakowski SM, Adler CM, Almeida J, et al. The functional neuroanatomy of bipolar disorder: a consensus model. *Bipolar Disord*. 2012;14(4):313-325.

37. Wechsler D. *Wechsler Adult Intelligence Scale–Revised (WAIS-R) Manual.* New York, NY: Psychological Corp; 1981.

38. Hamilton M. A rating scale for depression. *J Neurol Neurosurg Psychiatry*. 1960;23:56-62.

39. Young RC, Biggs JT, Ziegler VE, Meyer DA. A rating scale for mania: reliability, validity and sensitivity. *Br J Psychiatry*. 1978;133:429-435.

40. Lukoff D, Liberman RP, Nuechterlien KH. Symptom monitoring in the rehabilitation of schizophrenic patients. *Schizophr Bull*. 1986;12(4):578-602.

41. Lieberman MD, Cunningham WA. Type I and type II error concerns in fMRI research: re-balancing the scale. *Soc Cogn Affect Neurosci*. 2009;4(4):423-428.

42. Kiebel SJ, Holmes AJ. The general linear model. In: Frackowiak RS, Friston KJ, Frith CD, et al, eds. *Human Brain Function*. San Diego, CA: Elsevier Academic Press; 2007:101-126.

43. Penny WD, Stephan KE, Mechelli A, Friston KJ. Comparing dynamic causal models. *Neuroimage*. 2004;22(3):1157-1172.

44. Stephan KE, Penny WD, Moran RJ, den Ouden HEM, Daunizeau J, Friston KJ. Ten simple rules for dynamic causal modeling. *Neuroimage*. 2010;49(4):3099-3109.

45. Penny WD, Stephan KE, Daunizeau J, et al. Comparing families of dynamic causal models. *PLoS Comput Biol*. 2010;6(3):e1000709. doi:10.1371/journal.pcbi.1000709.

46. Mourão-Miranda J, Volchan E, Moll J, et al. Contributions of stimulus valence and arousal to visual activation during emotional perception. *Neuroimage*. 2003;20(4):1955-1963.

47. Pizzagalli DA, Lehmann D, Hendrick AM, Regard M, Pascual-Marqui RD, Davidson RJ. Affective judgments of faces modulate early activity (approximately 160 ms) within the fusiform gyri. *Neuroimage*. 2002;16(3, pt 1):663-677.

48. Bar M, Kassam KS, Ghuman AS, et al. Top-down facilitation of visual recognition [published correction appears in *Proc Natl Acad Sci U S A*. 2006;103(8):3007]. *Proc Natl Acad Sci U S A*. 2006;103(2):449-454.

49. Vuilleumier P, Pourtois G. Distributed and interactive brain mechanisms during emotion face perception: evidence from functional neuroimaging. *Neuropsychologia*. 2007;45(1):174-194.

50. Keil A, Costa V, Smith JC, et al. Tagging cortical networks in emotion: a topographical analysis. *Hum Brain Mapp*. 2012;33(12):2920-2931.

51. Gregoriou GG, Gotts SJ, Zhou H, Desimone R. High-frequency, long-range coupling between prefrontal and visual cortex during attention. *Science*. 2009;324(5931):1207-1210.

52. Delvecchio G, Sugranyes G, Frangou S. Evidence of diagnostic specificity in the neural correlates of facial affect processing in bipolar disorder and schizophrenia: a meta-analysis of functional imaging studies. *Psychol Med*. 2013;43(3):553-569. doi:10.1017/S0033291712001432.

53. O'Donnell BF, Hetrick WP, Vohs JL, Krishnan GP, Carroll CA, Shekhar A. Neural synchronization deficits to auditory stimulation in bipolar disorder. *Neuroreport*. 2004;15(8):1369-1372.

54. Özerdem A, Güntekin B, Atagün I, Turp B, Başar E. Reduced long distance gamma (28-48 Hz) coherence in euthymic patients with bipolar disorder. *J Affect Disord*. 2011;132(3):325-332.

55. Rass O, Krishnan G, Brenner CA, et al. Auditory steady state response in bipolar disorder: relation to clinical state, cognitive performance, medication status, and substance disorders. *Bipolar Disord*. 2010;12(8):793-803.

56. Liu TY, Hsieh JC, Chen YS, Tu PC, Su TP, Chen LF. Different patterns of abnormal gamma oscillatory activity in unipolar and bipolar disorder patients during an implicit emotion task. *Neuropsychologia*. 2012;50(7):1514-1520.

57. Frangou S. Brain structural and functional correlates of resilience to bipolar disorder. *Front Hum Neurosci*. 2011;5:184. doi:10.3389/fnhum.2011.00184.

58. Cotter D, Hudson L, Landau S. Evidence for orbitofrontal pathology in bipolar disorder and

major depression, but not in schizophrenia. *Bipolar Disord*. 2005;7(4):358-369.

59. Pantazopoulos H, Lange N, Baldessarini RJ, Berretta S. Parvalbumin neurons in the entorhinal cortex of subjects diagnosed with bipolar disorder or schizophrenia. *Biol Psychiatry*. 2007;61(5):640-652.

60. Berk M, Kapczinski F, Andreazza AC, et al. Pathways underlying neuroprogression in bipolar disorder: focus on inflammation, oxidative stress and neurotrophic factors. *Neurosci Biobehav Rev*. 2011;35(3):804-817.

61. Michel TM, Pülschen D, Thome J. The role of oxidative stress in depressive disorders. *Curr Pharm Des*. 2012;18(36):5890-5899.

62. Powell SB, Sejnowski TJ, Behrens MM. Behavioral and neurochemical consequences of cortical oxidative stress on parvalbumin-interneuron maturation in rodent models of schizophrenia. *Neuropharmacology*. 2012;62(3):1322-1331.

63. Cunningham MO, Whittington MA, Bibbig A, et al. A role for fast rhythmic bursting neurons in cortical gamma oscillations in vitro. *Proc Natl Acad Sci U S A*. 2004;101(18):7152-7157.

64. Moskvina V, Craddock N, Müller-Myhsok B, et al. An examination of SNP selection prioritization strategies for tests of gene-gene interaction. *Biol Psychiatry*. 2011;70(2):198-203.

65. Lewis DA, Curley AA, Glausier JR, Volk DW. Cortical parvalbumin interneurons and cognitive dysfunction in schizophrenia. *Trends Neurosci*. 2012;35(1):57-67.